Interfacial fatigue stress in PVD TiN coated tool steels under rolling contact fatigue conditions

Carvalho, N.J.M.; Huis in 't Veld, A.J.; Hosson, J.Th. De

Published in:
Surface & Coatings Technology

DOI:
10.1016/S0257-8972(98)00466-6

Publication date:
1998

ELSEVIER

Surface and Coatings Technology 105 (1998) 109–116

SURFACE & COATINGS TECHNOLOGY

Interfacial fatigue stress in PVD TiN coated tool steels under rolling contact fatigue conditions

N.J.M. Carvalho [a], A.J. Huis in 't Veld [b], J.Th. De Hosson [a,*]

[a] *Department of Applied Physics, Materials Science Centre, University of Groningen, Nijenborgh 4, 9747 AG Groningen, The Netherlands*

[b] *Department of Surface Engineering, TNO Institute of Industrial Technology, Laan van Westenenk 501, Postbus 541, 8300 AM Apeldoorn, The Netherlands*

Received 18 December 1997; accepted 27 January 1998

Abstract

Titanium–nitrogen (TiN) films were Physical Vapour Deposited (PVD) on tool steel substrates with different hardness and surface roughness, in a Bai 640R unit using a triode ion plating (e-gun) with a high plasma density. The coated substrates were submitted to a rolling contact fatigue test technique (modified pin-on-ring test) to obtain some clarifications of the mechanism of interfacial failure. Tests were run using PVD-coated rings finished by polishing or grinding to produce different surface roughnesses. From the results, it appears that the fatigue durability is at lower stress levels significantly influenced by both the pre-treatment and the final surface roughness of the material. The polished and smoother surfaces are associated with a longer fatigue life. However, at a higher contact stress, there appears to be very little influence of pre-treatment and surface roughness. Two mechanisms of crack propagation under pure rolling conditions were found, depending on the substrate hardness. For the softer substrates, the cracks propagate mainly perpendicular to the surface, whereas for the harder substrate, the cracks generally originate at the interface and progress in the coating parallel to the surface. © 1998 Elsevier Science S.A.

Keywords: Interfacial fatigue stress; Monolayers; Physical vapour deposition; Rolling contact fatigue; TiN coatings

1. Introduction

During the last few years, there has been increasing interest in titanium–nitrogen (TiN) due to its successful use in a variety of thin film applications. For example, the high degree of hardness of TiN makes it a particularly useful material for increasing the wear resistance of high-speed steel-cutting tools [1,2], punches [2], and metal-forming tools [1,2]. In addition, the good corrosion and erosion resistance of TiN, its relative inertness, high sublimation temperature, optical and electronic properties have resulted in TiN coatings, consideration for use as diffusion barriers in microelectronic devices [3], cosmetic gold-coloured surfaces [4], and wavelength-selective transparent optical films [5].

TiN has a cubic NaCl-type crystal structure with a lattice constant (for stoichiometric material) of 0.4340 nm and a vacancy defect structure that is stable over a wide composition range ($0.6 < N/Ti < 1.2$) [6]. Stoichiometric, as well as off-stoichiometric, polycrystalline TiN films have been deposited by a variety of techniques including reactive d.c. [7], r.f. [8], magnetron sputtering [9], activated evaporation [10], and triode ion plating (e-gun) with a high plasma density [11]. The observed physical properties of these films can vary over several orders of magnitude, depending on both the growth technique and the particular deposition parameters.

PVD TiN films were deposited on tool steel substrates with different hardnesses and surface roughnesses, in a Bai 640R unit using a triode ion plating (e-gun) with a high plasma density. Since the performance of a coated material is dependent on good coating adhesion, the measurement of this interface property is of considerable practical importance. The coated substrates are submitted to a rolling contact test technique to obtain some clarification on the mechanism of interfacial failure. This mechanism can be characterised by understanding the interrelation between surface roughness, surface hardness, contact stress and fatigue durability. Moreover, the understanding of different types of fatigue

* Corresponding author. Tel: +31 50 363 4898; Fax: +31 50 363 4881; e-mail: hossonj@phys.rug.nl

PII S0257-8972(98)00466-6

crack growth mode can give an insight into the coating–substrate bonding.

The advantage of this technique over scratch and indentation tests is that the critical load is a sensitive measure of the bonding conditions at the coating–substrate interface and it remains insensitive to the testing conditions [12].

In this report, we present results of an investigation of the TiN coating on tool steel substrate using Light Microscopy (LM) and Scanning Electron Microscopy (SEM).

2. Experimental

2.1. Specimen preparation

Two hardened and tempered alloy steels (tool steel) with hardnesses 50 and 60 HRc were used as substrate materials to investigate the influence of the hardness of the substrate in a rolling contact fatigue test.

The substrate surface was prepared by grinding or polishing. It is evident that the state of the substrate surface before coating has a strong influence on the bonding strength of hard coatings [13]. Different pre-treatments of the surface will generally lead to a difference in the resultant adhesion strength. Table 1 summarises the relevant details of the coating–substrates systems tested. With the purpose of analysing the influence of the coating deposition process, each system has two identical rings.

2.2. PVD TiN coating process

The Physical Vapour Deposition (PVD) TiN coatings investigated were deposited in a BAI 640R unit, which has a specially developed deposition process based on the standard Balzers TiN process, using a triode ion plating (e-gun) with high plasma density.

The PVD technique is an atomic deposition process at a relatively low temperature. Prior to deposition, the coating chamber is normally exhausted to high vacuum. In the case of wear protective coatings, the deposition temperature is 480 °C, and the operating pressure is normally in the range of 10^{-4}–10^{-2} Torr. In addition, if a negative substrate voltage (bias) is applied to the substrates, it is possible to sputter-clean (etch), i.e. remove, any oxides and impurity atoms on the surface before and during coating deposition. Consequently, plasma-assisted PVD provides coatings that reproduce the original substrate surface with a thickness of 2–5 μm. These coatings are also very dense, have few defects, and possess a good adhesion to the substrate.

The TiN coatings are gold–yellow-coloured and have a microhardness of 2300 HV (25 gram).

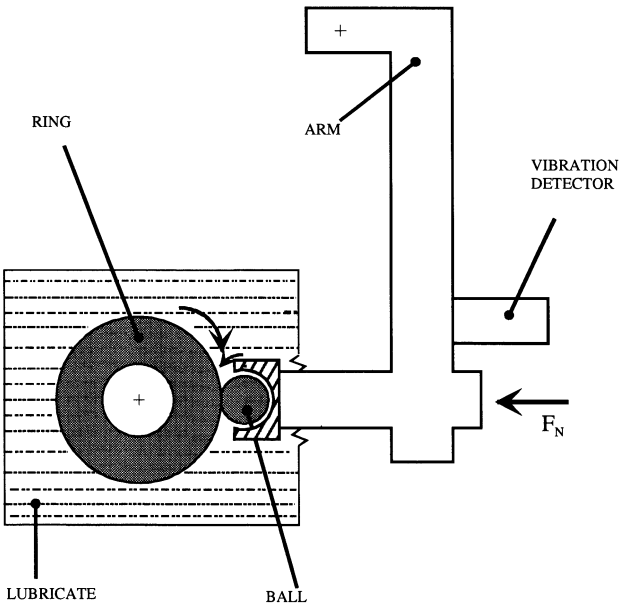

Fig. 1. Rolling ball-on-cylinder equipment (modified pin-on-ring tester).

2.3. The ball-on-ring tester

With the aim analysing the adhesion strength of the coating under conditions of dynamic loading, rolling

Table 1
Coating–substrates composites tested

Material group	Test piece	Tempering temperature	Pre-treatment	Roughness[a] R_a (μm)
I	1-1	600 °C/50 HRc	Polishing	0.03 ± 0.01
	1-2			
II	2-2	520 °C/60 HRc	Polishing	0.03 ± 0.01
	2-2			
III	3-1	520 °C/60 HRc	Polishing	0.15 ± 0.01
	3-2			
IV	4-1	520 °C/60 HRc	Grinding	0.10 ± 0.02
	4-2			

[a]The surface roughness data were obtained before coating deposition.

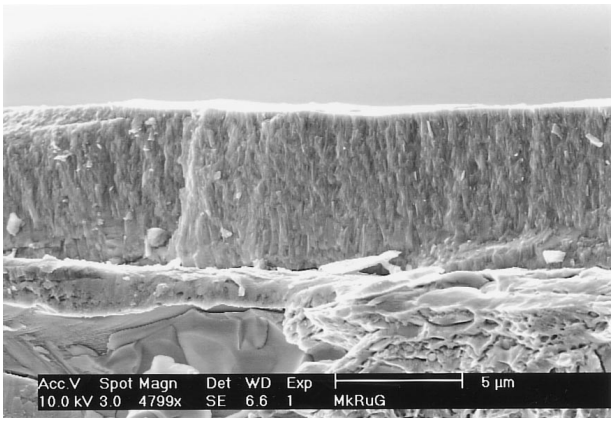

Fig. 2. Cross-sectional view of TiN coating on tool steel substrate. The coating–substrate composite is from material group III, which has the higher surface roughness.

contact fatigue tests have been carried out with a modified pin-on-ring tester, shown schematically in Fig. 1.

All tests were carried out under mineral-oil-lubricated conditions. Contact was achieved by pressing a ball, made of commercially available tungsten carbide with a radius of curvature $R=8$ mm, against the outer diameter of the ring under a known normal load F_N. This normal load F_N was applied through a pneumatic loading device ("pressure unit"), not shown in the drawing, its tension ranging from 0.4–1.2 kN. In such a load range, bulk plastic deformation did not occur in the specimens according to contact stress analysis using the classical Hertzian theory [14].

The ball rotates in a bronze socket along a fixed axis parallel to the axis of rotation of the ring, resulting in a pure rolling motion of the ball. During the test, the ring rotates against the ball at a speed of 500 rev min^{-1}, which corresponds to a surface speed of 1.6 m s^{-1}.

A vibration detector is mounted on the lever arm detecting the surface deterioration as a result of surface fatigue. The test stops when the vibration level increases 15%.

As tungsten carbide has a very high resistance against surface fatigue, the ball will usually survive many tests. Still, as a rule, for each test, a new ball is used. By shifting the ring in the axial direction between tests, it is possible to perform more tests per ring.

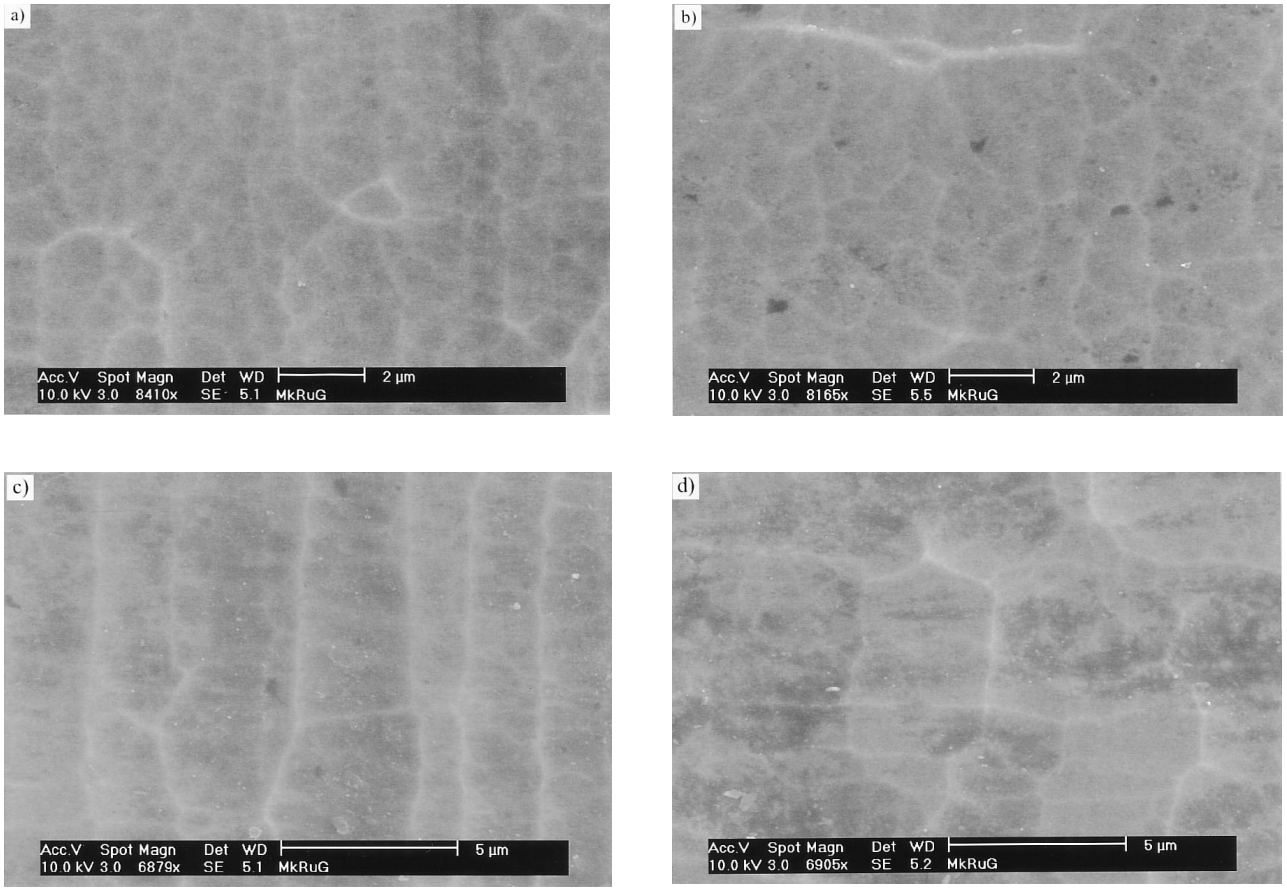

Fig. 3. Top view surface morphology of the coatings in a region free of rolling contact fatigue tests. The micrographs a, b, c and d correspond to the material groups I, II, III and IV, respectively.

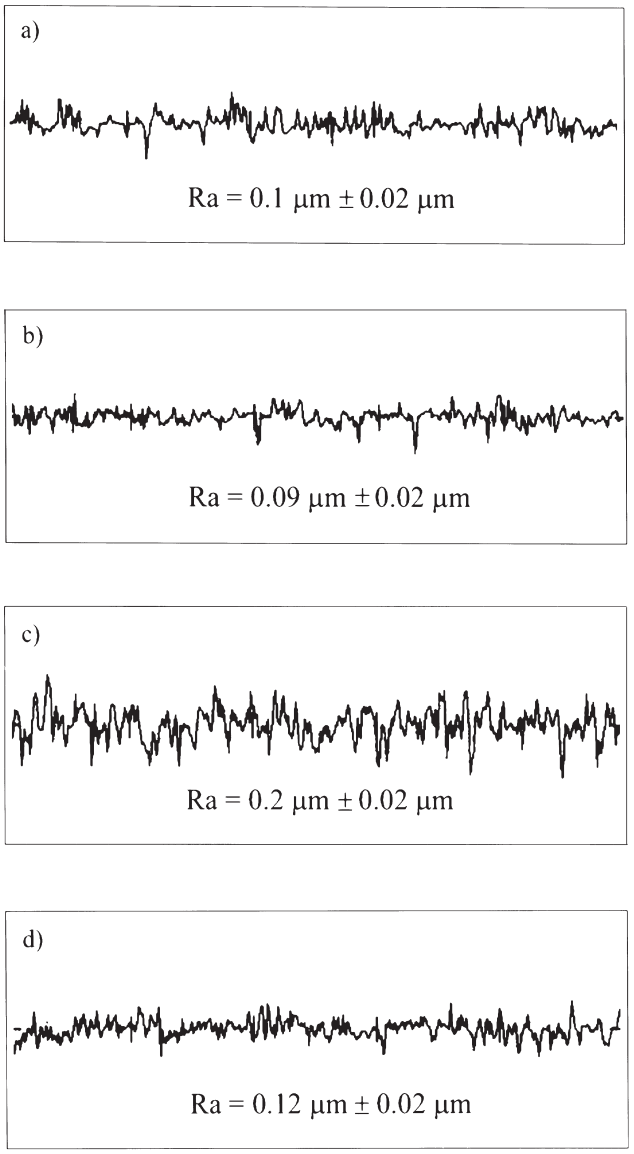

Fig. 4. Surface roughness of the coated rings in axial direction, a, I; b, II; c, III; d, IV. The coatings deposited on a polished pre-treated surface (a, b and c) have a slight increase in surface roughness, whereas the coatings deposited on the ground pre-treated surface (d) have a similar roughness.

3. Results

The thickness of the coatings was measured on polished cross-sectional samples, having values between 5 and 6 μm. The micrograph in Fig. 2 is a cross-sectional view of TiN in tool steel substrate. This specimen was obtained by cleaving the sample cooled in liquid nitrogen. As can be seen, the coating reproduces the original substrate surface and exhibits a columnar microstructure with dense grain boundaries.

The surface morphology and the surface roughness data (R_a values) of the coatings obtained for each of the four material groups are shown in Figs. 3 and 4, respectively. The coatings from material groups I and II have an identical surface morphology, consisting of small grains. The slight waviness and parallel lines on the surface of the coatings in material group III are due to the high surface roughness of the substrate. The surface morphology of the coatings from material group IV consists of a larger substructure than the coatings of material groups I and II, presumably due to the grinding present in pre-treatment.

3.1. Fatigue durability

The first tests were run on bare specimens without any coating under a normal stress of 5.1 GPa. No signs of contact fatigue cracks were found, and the bulk material did not suffer from pitting (surface fatigue) or spalling (subsurface fatigue).

Results from the rolling contact fatigue tests on coated specimens are shown in Fig. 5 with different pre-treatments and surface roughness and in Fig. 6 with different substrate hardnesses. In all the tests, the friction coefficient f varied from test to test, but all values were within the same range. The small variation of the data points obtained in Figs. 5 and 6 indicates that the variation of f had no significant influence on the test results, giving a good reproducibility of the tests.

All rings were submitted to three different contact stress: 3.5 GPa, 4.6 GPa and 5.1 GPa. From these results, it appears that the fatigue durability is significantly influenced both by the pre-treatment and the surface roughness of the substrate. It can be seen that at lower stress levels, the pre-treatment and the surface roughness of the rings have a large influence on the fatigue life with the polished smoother surface associated with a longer life. However, at the highest contact stress, there appears to be very little influence of pre-treatment and surface roughness.

The material group with higher substrate hardness has a typical relationship between contact stress and critical number of cycles for coating failure, although the material group with softer substrates has lower revolutions to failure for the lower contact stress.

3.2. Macroscopic nature of fatigue failures

Fig. 7 shows light microscope photographs of typical specimen failures for the four groups of test specimens. The specimens of group I, a material having a softer substrate, tend to fail in small regions transversal to the rolling direction. The specimens of group II tend to fail almost simultaneously around the entire circumference of the rolling path for a lower stress level, 3.1 GPa. For higher stress levels, the failure occurs at isolated points on the circumference.

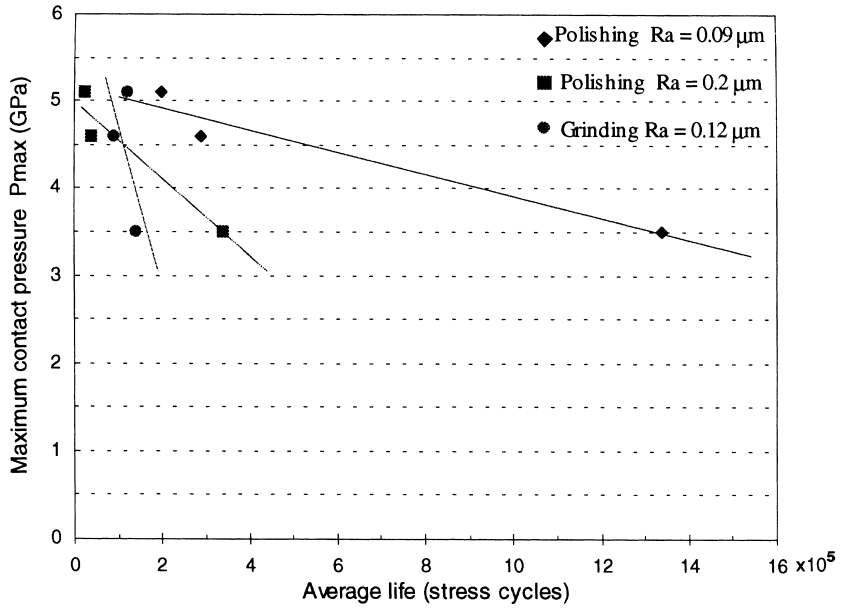

Fig. 5. Effect of surface roughness and pre-treatment on rolling fatigue.

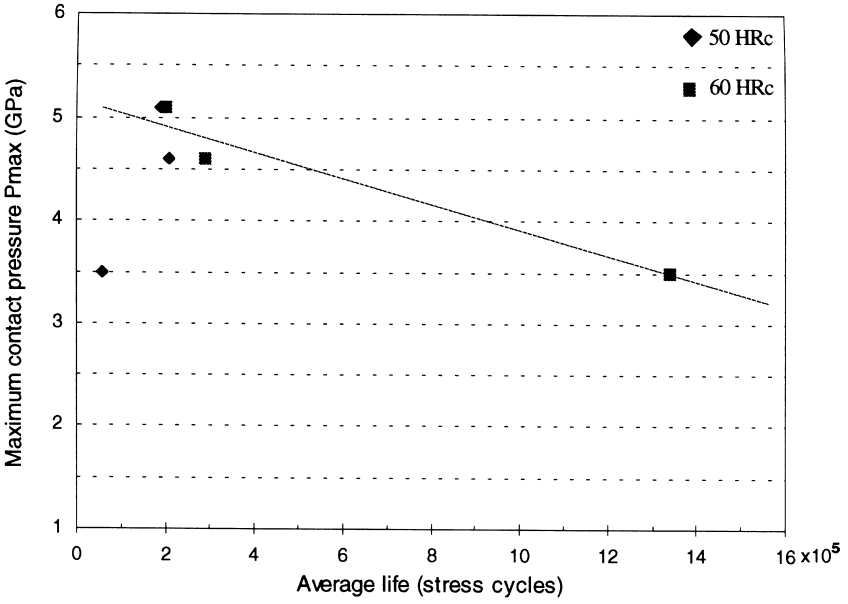

Fig. 6. Effect of substrate hardness on rolling fatigue.

Isolated fatigue pits usually appear in specimens of the other two materials, groups III and IV, for all the stress levels applied. The number of fatigue pits usually increases for the lower stress level. These differences in the number of sites may be due to differences in the probability of occurrence of cracks and in the speed with which the cracks propagate. It appears that in groups III and IV, smaller and more isolated fatigue cracks initiate and grow faster than those in the specimens from group II.

At higher stress levels, the materials of group I undergo crack propagation, showing a curved trajectory, from the edges of the rolling path to the centre. Those cracks cover the entire circumference of the ring.

3.3. Origin and growth of fatigue cracks

Chang et al. [15] analysed the mechanisms of delamination and coating failure for several TiN coating thickness. They reported that, in their case, the major failure mode of coating rolling contact tests was interfacial debonding. From the experimental results, they believed that the interfacial cracks are the failure sources of coated contact, and the spalling initiation mechanism

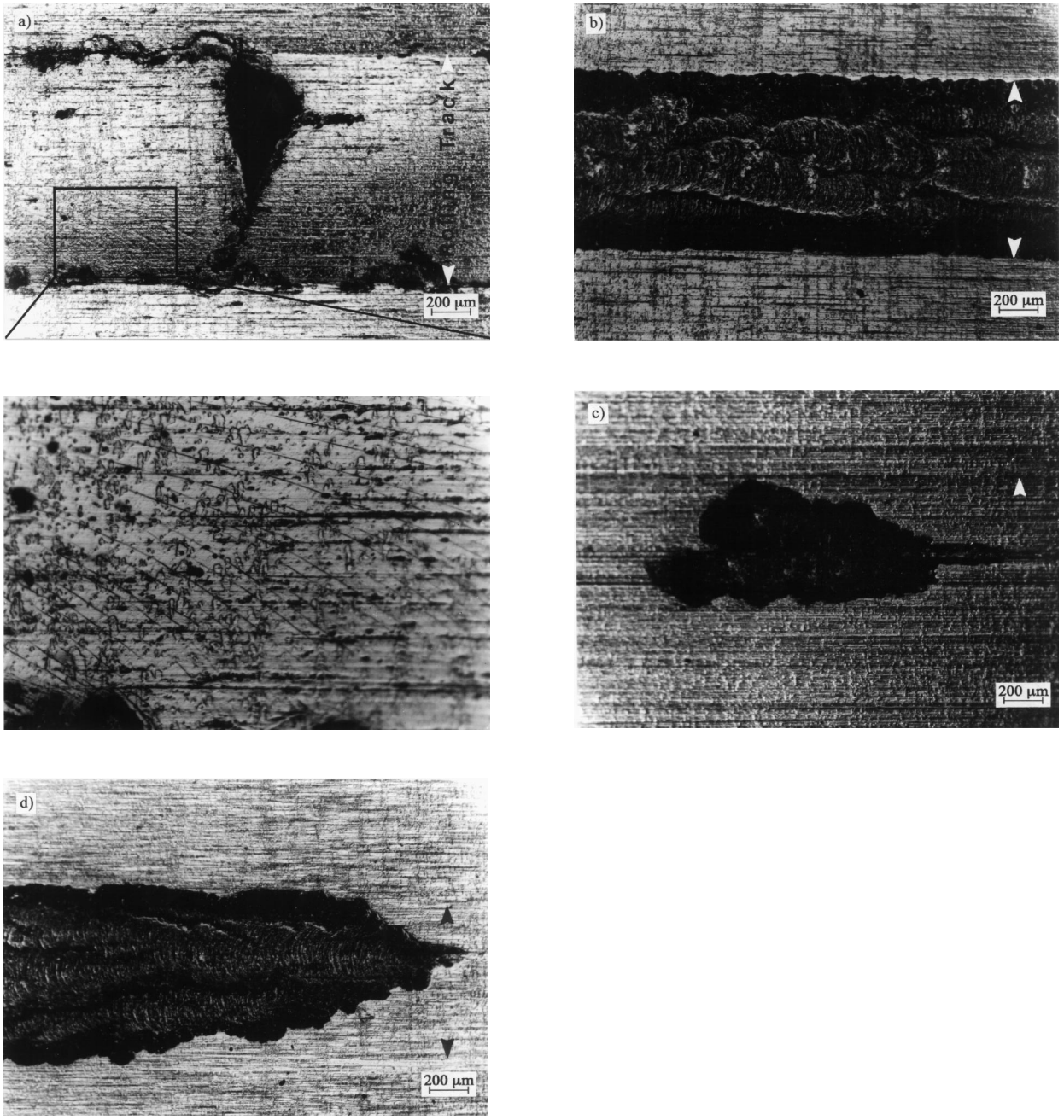

Fig. 7. Light microscopy photographs showing the different aspects of failure for the four groups of test rings: a, I; b, II; c, III; d, IV. The magnification of photograph a shows the cracks propagating to the centre of the rolling path.

originates from interfacial cracking leading to coating failure.

Scanning electron microscope micrographs of fatigue cracks appearing in all four material groups tested are shown in Fig. 8. Micrograph a is from a specimen of material group I (softer substrate) illustrating the origin and propagation of cracks perpendicular to the surface. At a higher stress level value, 5.1 GPa, this pattern of cracks appears around the entire rolling path. The failure by spalling at this stress level is very small. Reducing the stress level (from 5.1 GPa to 4.6 GPa and 3.5 GPa), the number of fatigue cracks diminishes, and the number of spalling spots increases.

In the other material groups, the cracks are generally initiated at the interface and grow in the coating parallel to the surface [see micrograph Fig. 8(c)]. When subcracks are formed and grow perpendicular to the interface, a small piece of material is released, resulting in the so-called spalling failure, as can be seen in micrograph Fig. 8(d). The amount and size of spalling failure spots increase with increasing stress level. This appears to show that the spalling initiation phenomenon

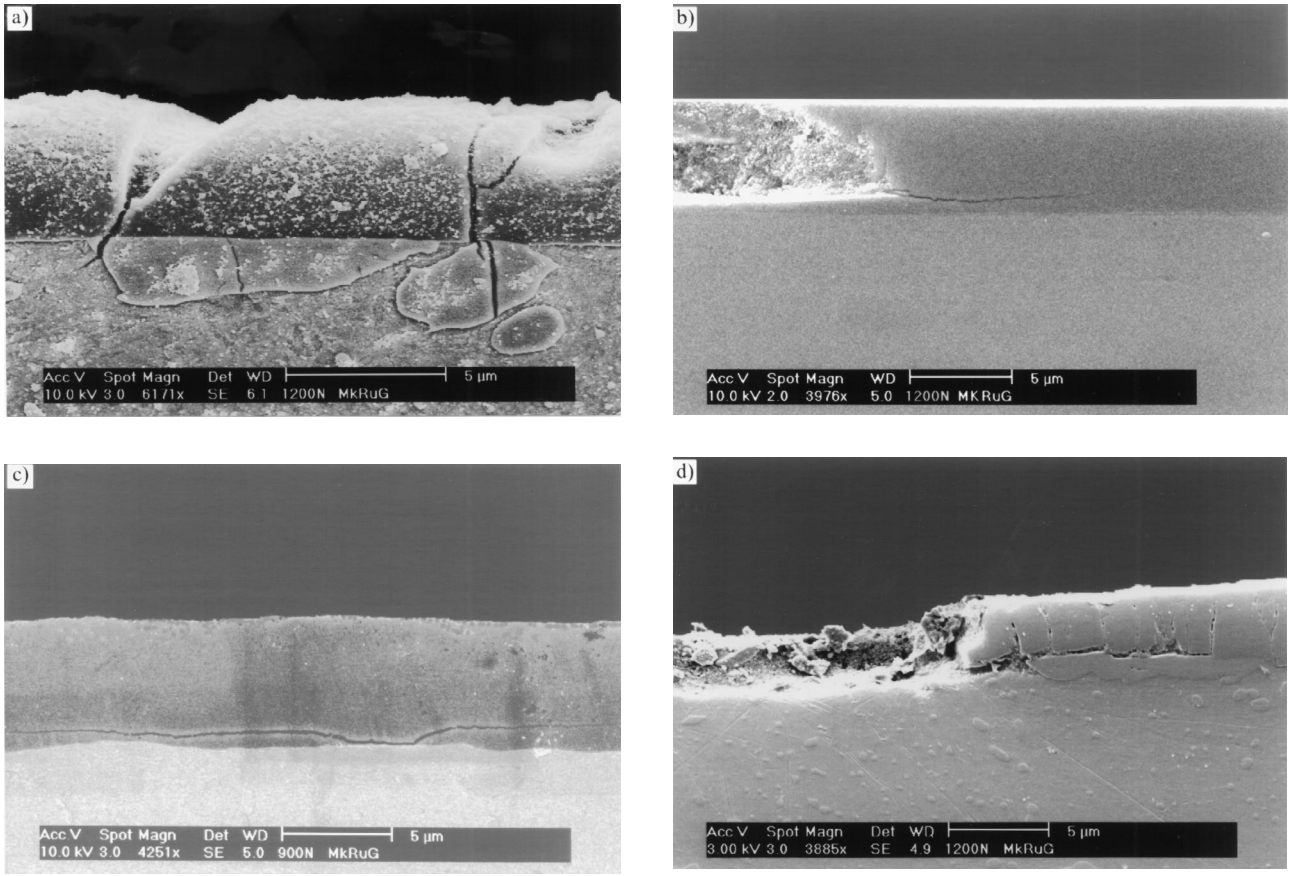

Fig. 8. Cross-sectional SEM micrographs showing the failure modes of the four material groups: a, I; b, II; c, III; d, IV. The micrographs were taken from polished coating–substrates composites.

of the present study is similar to the behaviour analysed by Chang et al. [15].

4. Discussion

From the experimental results it is clear that under the present testing conditions, fatigue failure of the coating–substrate composites is initiated at the interface region, and the interfacial failure stress, σ_c, is closely associated with the coating–substrate bonding conditions. Indeed, such factors as smooth substrate surface and polishing before coating, which are known to substantially improve the coating–substrate bonding strength [16], also improve the interfacial failure stresses. Fig. 5 shows the effect of surface finishing in interfacial failure stress. The σ_c of the polished surface is higher than that of the ground one. This implies that the shear strength in the interface region is increased when the mechanical bonding is improved, and the value of interfacial failure stress increases.

These results are in agreement with the analysis of contact mechanics, which shows that the shear stress range $\Delta\tau_{zx}$ at the interface is the appropriate parameter that should be used to characterise the interfacial failure stress and cyclic bonding strength of hard coatings [12].

Theoretically, the coating–substrate adhesion strength is determined by the interfacial structure and bonding conditions and is independent of intrinsic properties such as hardness of the coating and substrate [12]. However, as can be seen in Ref. [17] and in Fig. 6, the substrate hardness influences the interfacial failure stress under cyclic loading. This can be explained, using the assumption that for softer substrates, at higher loads, the substrate reduces the stress of the system by elastic deformation and increases the stress level in the coating. The result is a crack initiation in the PVD layer or in the interface and propagation perpendicular to the surface. At lower loads, the substrate does not deform, and stress is released by spalling fatigue failure.

Chang et al. [15] examined the progressive damage of the contact surfaces by recording the surface morphology as contact continued. They plotted the spalling area as a function of the contact cycle of the coated roller. The curve revealed a slow propagation phase followed by a fast growth to failure of the coated roller. This process of crack initiation and growth can be explained using the model developed by Otsuka et al. [18]. The

first stage of damage is the formation of fine mode II cracks parallel to the contact surface that are created by the cyclic shear component of the contact stress. The next stage consists of fast growth of the initial fine cracks into macroscopic cracks both by extension of themselves and by coalescence with neighbouring cracks as stress cycling continues. The final result is a surface distress spalling fatigue failure along these extended cracks. This model is also in agreement with the theory of stress shadow.

Differences in the growth mode of cracks of the materials tested, can be related to differences in microplastic deformation, which are most likely responsible for the observable macroplastic deformation and fatigue behaviour differences.

5. Conclusions

The following may be concluded from the above discussion.

(1) A small number of tests for each case were performed, but a good reproducibility was obtained. Therefore, conclusions can be drawn from the results.
(2) Bare specimens without any coating were tested under the same applied load as the coated ones, and no pitting or spalling of the bulk materials had occurred. Therefore, this experimental method seems to be reliable for determining the cyclic bonding strength.
(3) Considerable differences in fatigue durability were found among systems with equivalent chemical composition, macro- and microstructure and mechanical properties when differences exist in surface finishing and surface roughness. These results reveal the dependence of rolling contact fatigue on the pretreatment and surface roughness.
(4) In the case of systems with a softer substrate, the interfacial failure stress cannot be well quantified by rolling contact fatigue tests because this test is only sensitive to fatigue cracks that lead to spalling failure.
(5) Interfacial fatigue strength is a significant measure of the adhesion between film and substrate, since it is sensitive to the interface condition (pretreatment).

Acknowledgement

The work described in this paper has been supported by TNO Institute of Industrial Technology. The authors acknowledge Balzers Group for the deposition of PVD TiN coatings on tool steel rings and Emile van der Heide for his assistance and discussion on the rolling contact fatigue tests.

References

[1] R. Buhl, H.K. Pulker, E. Moll, Thin Solid Films 80 (1981) 265.
[2] R.L. Hatschek, Am. Mach. Special Report No. 752, March, 1983, p. 129.
[3] M. Wittmer, B. Studer, H. Melchiar, J. Appl. Phys. 52 (1981) 5722.
[4] B. Zega, M. Kornmann, J. Amiguet, Thin Solid Films 54 (1977) 577.
[5] E.T. Valkonen, Karlsson, B. Karlsson, B.O. Johansson, Proc. SPIE Int. Technical Conf. Vol. 401, 1983, p. 41.
[6] L.E. Toth, Transition Metal Carbides and Nitrides, Academic, New York, 1971, p. 118.
[7] J.M. Poitevin, G. Lemperier, J. Tardy, Thin Solid Films 97 (1982) 69.
[8] J.-E. Sundgren, B.O. Johansson, S.-E. Sundgren, U. Helmersson, Thin Solid Films 122 (1984) 115.
[9] M.K. Hibbs, B.O. Johansson, J.-E. Sundgren, U. Helmersson, Thin Solid Films 122 (1984) 115.
[10] B.E. Jacobson, R. Nimmergadda, R.F. Bunshah, Thin Solid Films 63 (1979) 333.
[11] M. Bromark, M. Larsson, P. Hedenqvist, S. Hogmark, Surf. Coat. Technol. 90 (1997) 217.
[12] J.-W. He, B.C. Hendrix, N.-S. Hu, Surf. Eng. 12 (1996) 49.
[13] H. Chen, M.-Z. Y, K.-W. Xu, J.-W. He, Surf. Coat. Technol. 7475 (1995) 253.
[14] J.W.M. Mens, C.A. Boose, A.W.J. de Gee, Tribol. Int. 24 (1991) 351.
[15] T.P. Chang, H.S. Cheng, W.D. Sproul, Surf. Coat. Technol. 4344 (1990) 699.
[16] R.S. Gao, C.D. Bai, K.-W. Xu, J.-W. He, R. Soc. Chem. 2 (1993) 285.
[17] R. Thom, L. Moore, W.D. Sproul, T.P. Chang, Surf. Coat. Technol. 62 (1993) 423.
[18] A. Otsuka, H. Sugawara, M. Shomura, Fatigue Fract. Eng. Mater. Struct. 19 (1996) 1265–1275.